

# The Effect of pH on the Properties of Hydrothermally Synthesized CeO<sub>2</sub> Nanoparticles

Yasir Saleem Yaseen <sup>1, a\*</sup>, Ghassan Adnan Naeem <sup>2, b</sup>

<sup>1</sup>Department of physics, College of Education for Pure Science, University of Anbar, Ramadi, Iraq,

<sup>2</sup> Department of Medical Physics College of Applied Science-Hit University of Anbar Hit, 31007 Anbar, Iraq.

## Abstract

In this study CeO<sub>2</sub> NPs were successfully prepared via the hydrothermal method and influence of pH on the properties . The prepared nano-sized particles were characterized using various techniques including: Ultraviolet-Visible (UV-Vis) spectroscopy, X-ray diffraction (XRD), Field Emission Scanning Electron Microscopy (FESEM), Energy-Dispersive X-ray spectroscopy (EDX). The (UV-Vis) spectra showed the absorption peak changing from 335 nm to 298 nm with increasing pH value from 7 to 11, indicating the occurrence of a blue shift, which is a prior indication of the decrease in the grain size of CeO<sub>2</sub> nanoparticles with increasing pH value. The XRD pattern of CeO<sub>2</sub> NPs reveals the fluorite cubic structure, the crystallite size changes with an increase in pH value. According to FETEM image analysis, the average CeO<sub>2</sub> particle size decreases from 35.85 to 20.65 nm with increasing pH value from 7 to 11. Energy Dispersive X-ray analysis (EDX) was utilized to determine the constituent elements of CeO<sub>2</sub> NPs mixture.

**Keywords:** Cerium oxide nanoparticles, Hydrothermal synthesis, pH influence, Nanoparticle synthesis, Catalytic applications.

## تأثير الرقم الهيدروجيني على خواص الجسيمات النانوية Ce O<sub>2</sub> المصنعة بالطريقة الحرارية المائية

ياسر سليم ياسين <sup>1\*</sup>, غسان عدنان نعيم <sup>2</sup>

<sup>1</sup>قسم الفيزياء، كلية التربية للعلوم الصرفة، جامعة الأنبار، الأنبار، العراق

<sup>2</sup>قسم الفيزياء الطبية، كلية العلوم التطبيقية، جامعة الأنبار، الأنبار، العراق

### الخلاصة

في هذه الدراسة تم تحضير CeO<sub>2</sub> NPs بنجاح عبر الطريقة الحرارية المائية وتأثير الرقم الهيدروجيني على الخصائص. تم تشخيص الجسيمات النانوية المحضرة باستخدام تقنيات مختلفة بما في ذلك: التحليل الطيفي للأشعة فوق البنفسجية والمرئية (UV-Vis)، حيود الأشعة السينية (XRD)، المجهر الإلكتروني الماسح ذو الانبعاثات الميدانية (FESEM)، التحليل الطيفي للأشعة السينية المشتتة للطاقة (EDX). أظهرت أطياف (UV - Vis) تغير ذروة الامتصاص بين 335 (nm - 298) مع زيادة قيمة الرقم الهيدروجيني PH من 7 إلى 11، مما يشير إلى حدوث تحول إلى اللون الأزرق، وهو مؤشر مسبق على انخفاض الحجم الحبيبي لجزيئات CeO<sub>2</sub> النانوية. مع زيادة قيمة الرقم الهيدروجيني. يكشف نمط XRD لـ CeO<sub>2</sub> NPs عن البنية المكعبة للفلوريت، ويتغير حجم البلورات مع زيادة قيمة الرقم الهيدروجيني. وفقًا لتحليل صور FESEM، انخفض متوسط حجم جسيم CeO<sub>2</sub> من 35.85 nm إلى 20.65nm مع زيادة قيمة الرقم الهيدروجيني PH من 7 إلى 11. تم استخدام تحليل الأشعة السينية المشتتة للطاقة (EDX) لتحديد العناصر المكونة لخليط CeO<sub>2</sub> NPs.

## 1. Introduction

Nanoparticles (NPs) have become an integral part of contemporary research into various nanostructures. Over the past decade, these materials have received great attention in the fields of nanoscience and nanotechnology due to their important physical and chemical properties [1]. Nanotechnology deals with manipulating the size and shape of materials at the nano- scale to enrich their quality [2]. The aim of this reduction to nanoscale is to enhance the optical, electrical and biological properties which can be used in different applications from medicine to complex engineering, and physics to chemistry [3].

Industrial rare earth, a medicine for the industrial body in particular, has been used as a new material treasure, which promotes the technology progress of traditional industries and is widely used in the sector of information and biotechnology [4]. Rare earth compounds are characterized by their 4f orbital structure and exhibit unique surface properties that serve many physical, optical, and biological applications [5]. Among the rare earth group of rare earth oxides is cerium oxide ( $\text{CeO}_2$ ). The unique characteristics of cerium oxide  $\text{CeO}_2$  owing to its size, shape, and extended reactive surface area, including oxygen storage and release capabilities.  $\text{CeO}_2$  is characterized by oxygen ions occupying tetrahedral sites within a tight cubic packing of cerium ions [6]. The unique properties of cerium oxide result from its abundant surface defects, a large number of surface hydroxyl groups, and its redox potential. Redox promotes the high mobility of lattice oxygen, which is responsible for the catalytic properties of  $\text{CeO}_2$  [7]. In terms of properties, cerium oxide is a complex material of great interest for many areas of use. The physical properties of  $\text{CeO}_2$  depend on the pH conditions prevailing during preparation and thus affect the crystallization size and morphological structure [8]. Investigating the impact of pH on the properties of  $\text{CeO}_2$  nanoparticles helps to adapt the latter for different purposes. When changing the PH value, it leads to a change in the absorption of protons or hydroxyl groups and thus changes the surface charge density, i.e. a change in internal energy, and growth increases, which affects the shape, size, and distribution of nanostructures and morphology [9]. Various synthesis techniques, including the hydrothermal method, sol-gel, co-precipitation, spray Pyrolysis, sonochemical, ball-milling, and microemulsion, have been employed to fabricate  $\text{CeO}_2$  nanoparticles [10-15]. The hydrothermal method is a technique used to synthesize nanoparticles by utilizing high pressure and high temperature conditions in a closed container. Chemical reactions occur in an aqueous solution above the boiling point of water. Hydrothermal synthesis offers many advantages such as relatively mild operating conditions (reaction temperatures below 300 °C), one-step synthetic procedure, environmental friendliness, and good dispersion in solution. Furthermore, hydrothermal synthesis is inexpensive in terms of hardware, energy and precursor material the one that received the greatest amount of attention for being the simplest and the easiest to produce nanocrystalline  $\text{CeO}_2$  particles [16-18].

To our knowledge, This is the first study on the role of pH in the preparation of  $\text{CeO}_2$  nanoparticles using hydrothermal technique. The composition and morphology of  $\text{CeO}_2$

nanoparticles prepared using the hydrothermal method have been studied and explored as part of this research.

## 2. Experimental Method

The process of preparing CeO<sub>2</sub> NPs, shown in *Fig. (1)*, involves dissolving (4.34 g) cerium nitrate hexahydrate [Ce(NO<sub>3</sub>)<sub>3</sub> 6H<sub>2</sub>O] in (100 ml) of distilled water. At the same time, (2 g) of sodium hydroxide [NaOH] is dissolved in (500 ml) of distilled water. And add the sodium hydroxide solution drop by drop to the cerium nitrate solution with continuous stirring at room temperature until pH (7,11) is reached. Procedure Hydrothermal treatment at 150°C for 12 hours for the resulting solution which is placed in the autoclave. Leave the autoclave to lower the temperature to room temperature. Collect the subsequent milky residue, subject it to centrifugation, and use distilled water and ethanol to wash it multiple times. Dry the washed powder at a temperature of 60°C for 2 hours. Submit the dried powder to calcination for 4 hours at 240°C. The dried sample is subjected to calcination for 4 hours at 240°C.

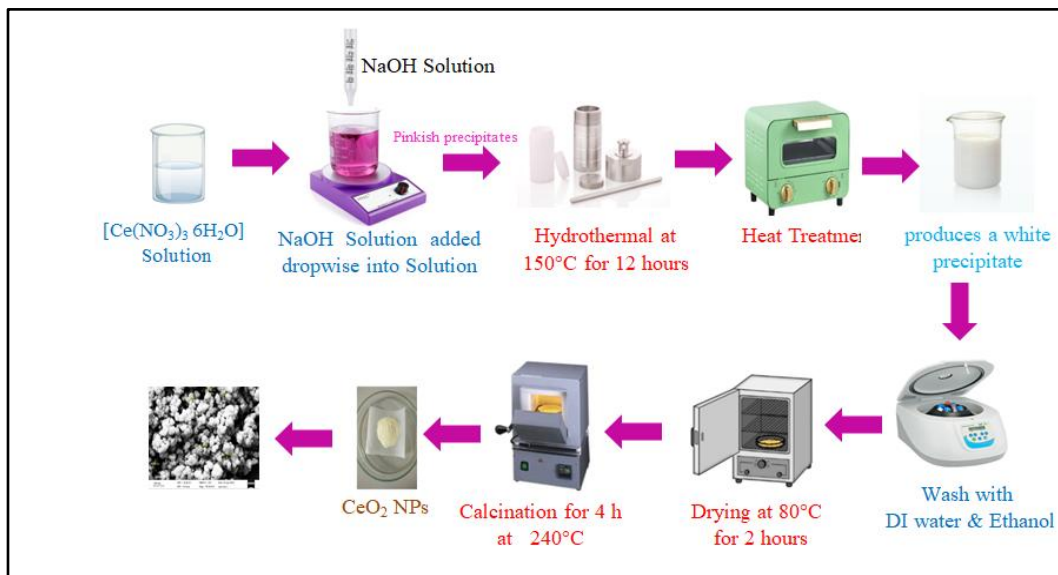


**Figure -1** Graphical representation of the manufacture of (CeO<sub>2</sub> NPs)

## 3. Characterizations

Optical transmittance was obtained for the studied materials in the wavelength range of 180–850nm by using a UV-visible spectrophotometer. Analysis results were obtained regarding the absorbance of substances and the possibility of using them as transparent materials for optical devices and other related research-ray diffraction (XRD) involving a Rigaku diffractometer with Cu K-radiation ( $\lambda=1.54187$ ) was used to investigate the structural properties of the samples at room temperature. Information on the crystalline structure of the synthesized products was obtained from XRD patterns that were taken in a wide range from 10 to 90 degrees. FESEM equipped with EDX for complete particle morphology and chemical composition evaluation. With

this approach, high-resolution images were obtained as well as maps showing the nature, sizes, and shapes of the nanoparticles.

#### 4. Results and Discussion:

Fig 2. displays the XRD pattern of the samples that were synthesized for pH values of 7, 8, 9, 10 and 11, it can be observed diffraction peaks at  $2\theta$  values ranging from  $30^\circ$  to  $80^\circ$  are:  $28.53^\circ$ ,  $33.05^\circ$ ,  $47.46^\circ$ ,  $56.33^\circ$ ,  $59.04^\circ$ ,  $69.40^\circ$ ,  $76.71^\circ$  and  $79.07^\circ$  indicate of crystalline planes, aligning with the Miller indices (111), (200), (220), (311), (222), (400), (331), and (420). The peaks corresponding to various crystallographic planes confirm the fluorite structure and face-centered cubic morphology of pure  $\text{CeO}_2\text{NPs}$ . The XRD patterns corresponds well with the reported data for  $\text{CeO}_2$  (JCPDS Card No. 34-0394) [19, 20]. The XRD patterns not only confirms the successful synthesis of  $\text{CeO}_2\text{NPs}$  but also highlights the impact of pH on the crystalline structure and size distribution. The decline in peak intensity as pH is increased may suggest that the precursor solutions' pH influences the nanoparticles crystallinity. This is consistent with previous studies that report differences PH during synthesis can result in changes in crystallite size and structural properties [21, 22]. Due to the increase in the full width at half-maximum (FWHM) for the prepared samples, the peak density is reduced. The broader peaks suggest a distribution of crystallite sizes within the synthesized  $\text{CeO}_2\text{NPs}$ . This phenomenon could be attributed to the influence of pH on the nucleation and growth processes during hydrothermal treatment, leading to variations in particle size [9, 21, 22].

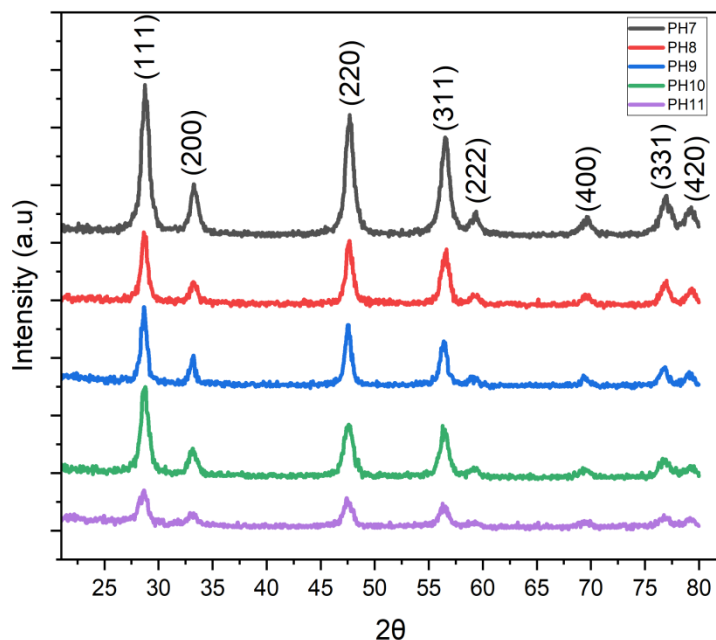


**Figure -2** XRD patterns of thermally prepared  $\text{CeO}_2\text{NPs}$  samples for different pH values.

The equation used to determine the crystallite size (D) of the nanostructured  $\text{CeO}_2\text{NPs}$  is the Scherrer-Debye equation (Scherrer-Debye Equation) [23]:

$$D = \frac{K\lambda}{\beta \cos \theta} \dots\dots\dots (1)$$

Here D is the crystallite size, λ represents the wavelength of Cu-Kα radiation, K is a constant with a value of 0.9, θ is the diffraction angle, and β is the full-width at half maximum (FWHM). The value of micro strain (ε) was calculated according to the equation [24]:

$$\epsilon = \frac{\beta_{0.5}}{4 \tan \theta} \dots\dots\dots (2)$$

The value for the dislocation intensity defect (δ) is obtained by means of the following formula. [25]:

$$\delta = \frac{1}{D^2} \dots\dots\dots (3)$$

The following formula was derived to estimate surface area of CeO<sub>2</sub>NPs [26]:

$$S.A. = \frac{6}{D_{av} \rho} \dots\dots\dots (4)$$

Where ρ represent density of CeO<sub>2</sub>NPs is (7.22 g/cm<sup>3</sup> ).

The estimated crystal size(D) using Scherer -Debye equation in addition to the micro strain (ε), dislocation density(δ) and surface area (S.A.) of the CeO<sub>2</sub> nanocrystals are listed in *Table (1)*.

**Table 1-** Structural parameters of CeO<sub>2</sub> Nan crystals

Value of pH	2θ	β	D(nm)	(δ) x 10 <sup>11</sup> /cm <sup>2</sup>	(ε) x 10 <sup>-3</sup>	(S.A.) x10 <sup>4</sup> cm <sup>2</sup> /g
PH7	28.6589	0.012	11.95	0.007	0.0117	69.54
PH8	28.6965	0.008	18.01	0.003	0.0078	46.14
PH9	28.6204	0.004	36.48	0.0007	0.0039	22.78
PH10	28.6098	0.010	14.44	0.004	0.0098	57.55
PH11	28.6836	0.006	23.9	0.0017	0.0058	34.77

From *Table (1)* it was shown that the increase in crystalline size for with increasing pH values (8,9) indicates that a more alkaline environment increases the width of the main peak and Crystal size values fluctuate with increasing pH values (10,11). This fluctuation in increase and decrease in crystalline size with increasing pH also indicates the controlling role of pH in the nucleation and crystal growth processes during the synthesis process. Allso it seen that the value of

dislocation density ( $\delta$ ), surface area (SA), and microstress values ( $\epsilon$ ) decreased for with increasing pH values(8,9) and fluctuate with increasing pH values (10,11). It is possible that the pH affects crystal growth negatively due to the increase in crystal size, so the surface area of the crystals decreases, and as a result of the decrease in the micro strain that the crystal exhibits as a result of its exposure to stress, so the dislocation density decreases accordingly.

Figure (4) shows UV-visible spectrum of thermally prepared CeO<sub>2</sub>NPs at different pH values (7, 8, 9, 10 and 11) . The observed absorption near-ultraviolet region arises from electronic transitions resulting from the phenomenon of surface plasmon resonance (SPR). We have observed that spectrum of CeO<sub>2</sub>NPs is characterized by peaks whose position is dictated by the pH value. We note that the location of the absorption peak is consistent with the peak location of cerium oxide nanoparticles from previous studies [15, 27].

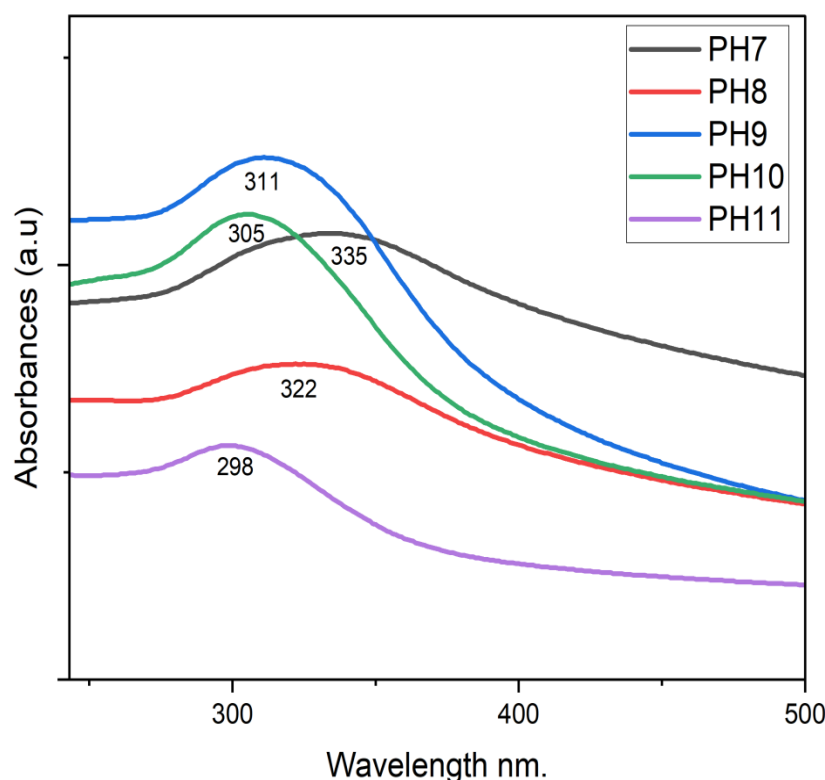


Figure -3 UV-Visible spectra of hydrothermally synthesized CeO<sub>2</sub> nanoparticles

From Table (2) it is observed the change of the location of the  $\lambda(\text{max})$  absorption peaks of the CeO<sub>2</sub>NPs ( $\lambda(\text{max})$ ) with an increasing pH. This shift is towards higher energy (lower wavelengths), which is a characteristic that indicates the reduction in CeO<sub>2</sub>NP size with an increasing pH value. This phenomenon suggests that the absorption sites are dependent on the shapes and sizes of the CeO<sub>2</sub> nanoparticles.

**Table 2-** UV–Vis data for CeO<sub>2</sub>NPs hydrothermally synthesized with varied values of pH

pH value	absorption peaks ( $\lambda(\text{max})$ )
pH=7	335
pH=8	322
pH=9	311
pH=10	305
pH=11	298

The morphology of ceria nanoparticles prepared using the hydrothermal approach from different pH value is illustrated in *Fig. (4)*. The FESEM analysis, further confirms that the cerium oxide nanoparticles had been successfully synthesized and it gives details about shape, size distribution, and dispersion. This analysis shows that heat treatment resulted in a lot of homogeneity of the surfaces of the samples. The nanoscale CeO<sub>2</sub> particles seen in the FESEM images have clearly defined spherical shapes.

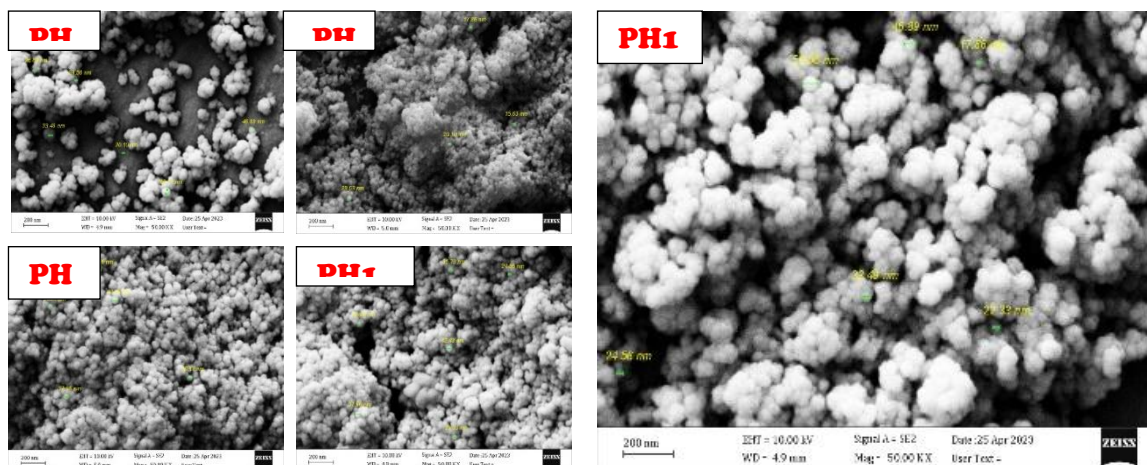


**Figure -4** Field Emission Scanning Electron Microscopy (FESEM) images of CeO<sub>2</sub>NPs hydrothermally at different values of pH

From *Fig. (4)*, it is seen that at pH values (7,8) the presence of the spherical shape demonstrates equal formation of nanoparticles that suggests the suitability of adopted hydrothermal method. We notice that the cerium oxide nanoparticles are decreases from 35.85 to 20.65 nm with increasing pH values. The increasing percentage of sodium hydroxide works to aggregate the cerium nanoparticles to give a nanostructure similar to a cauliflower flower, which increases their surface area, thus increasing their effectiveness, and this is consistent with many

previous studies [28, 29]. The agglomeration phenomenon is responsible the huge variation between crystallite size and grain size [30].

Fig. (5) shows the results of EDX analysis of the elemental composition of CeO<sub>2</sub> nanoparticles made by the hydrothermal method. The occurrence of cerium (Ce) and oxygen (O) peaks can be seen in the spectrum which prove to be a characteristic feature of the CeO<sub>2</sub> nanoparticles. It is noted that small peaks appear attributed to elements such as: gold (Au), aluminum (Al), and nitrogen (N), which give information about the impurities that interfere with the process of preparing CeO<sub>2</sub> nanoparticles.

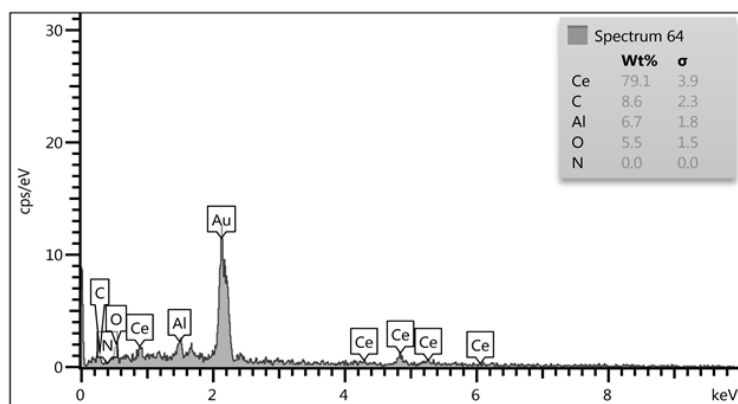


Figure -5 (EDX) analysis of CeO<sub>2</sub>NPs hydrothermally synthesized.

## 5. Conclusion:

In summary, CeO<sub>2</sub> nanoparticles were effectively produced by a simple hydrothermal process by using pH (7 - 11) from cerium nitrate hexahydrate [Ce (NO<sub>3</sub>)<sub>3</sub> 6H<sub>2</sub>O] solution with sodium hydroxide. The effects of pH on the structural and morphological characteristics of CeO<sub>2</sub> were examined systematically. the increase in crystalline size for with increasing pH values indicates that a more alkaline environment increases the width of the main peak and Crystal size values fluctuate with increasing pH values. This fluctuation in increase and decrease in crystalline size with increasing pH also indicates the controlling role of pH in the nucleation and crystal growth processes during the synthesis process. X-ray diffraction (XRD) analysis revealed that the synthesized CeO<sub>2</sub>, nanoparticles possess a fluorite structure and a face-centered cubic. nanoparticles is found to be altering between ~11 to 36 nm. The UV-Vis spectrum of the CeO<sub>2</sub> nanostructure showed that the pH value has an effective and influential role in determining the wavelength value ( $\lambda$  max) of the absorption peak resulting from the phenomenon of Surface Plasmon Resonance (SPR). The blue shift of absorption peak with increasing pH value is a prior indicator of the decrease of grain size in CeO<sub>2</sub> nanostructure. The results of (FESEM) emphasized the significant role of pH in changing particle shape is observed through the agglomeration of CeO<sub>2</sub> grains to obtain a nanostructure with granules with a cauliflower flower-like shap, The agglomeration phenomenon is responsible the huge variation between crystallite size and grain size.

**References**

- [1] Mustafa, F., M. Carhart, and S. Andreescu, *A 3D-printed breath analyzer incorporating CeO<sub>2</sub> nanoparticles for colorimetric enzyme-based ethanol sensing*. ACS Applied Nano Materials, 2021. **4**(9): p. 9361-9369.
- [2] Rabeea, M.A., et al., *Phytosynthesis of Prosopis farcta fruit-gold nanoparticles using infrared and thermal devices and their catalytic efficacy*. Inorganic Chemistry Communications, 2021. **133**: p. 108931.
- [3] Naeem, G.A., M.A. Majeed, and S.G. Khalil, *Improvement of Silver Nanoparticles Biosynthesized Using Various Quantities of Ruta Leaf Extract*. International Journal of Nanoscience, 2024. **23**(02): p. 2350060.
- [4] Xu, C. and X. Qu, *Cerium oxide nanoparticle: a remarkably versatile rare earth nanomaterial for biological applications*. NPG Asia materials, 2014. **6**(3): p. e90-e90.
- [5] Surendra, T. and S.M. Roopan, *Photocatalytic and antibacterial properties of phytosynthesized CeO<sub>2</sub> NPs using Moringa oleifera peel extract*. Journal of Photochemistry and Photobiology B: Biology, 2016. **161**: p. 122-128.
- [6] Matović, B., et al., *Influence of Mg doping on structural, optical and photocatalytic performances of ceria nanopowders*. Processing and Application of Ceramics, 2017. **11**(4): p. 304-310.
- [7] Ederer, J., et al., *Nanocrystalline cerium oxide for catalytic degradation of paraoxon methyl: Influence of CeO<sub>2</sub> surface properties*. Journal of Environmental Chemical Engineering, 2021. **9**(5): p. 106229.
- [8] Zhou, Y. and M. Rahaman, *Hydrothermal synthesis and sintering of ultrafine CeO<sub>2</sub> powders*. Journal of materials research, 1993. **8**(7): p. 1680-1686.
- [9] Malligavathy, M. and D. Pathinettam Padiyan, *Role of pH in the hydrothermal synthesis of phase pure alpha Bi<sub>2</sub>O<sub>3</sub> nanoparticles and its structural characterization*. Adv. Mater. Processes, 2021. **2**: p. 51-55.
- [10] Abd-Alghafour, N., et al., *Fabrication and characterization of ethanol gas sensor based on hydrothermally grown V<sub>2</sub>O<sub>5</sub> nanorods*. Optik, 2020. **222**: p. 165441.
- [11] Yulizar, Y., et al., *Novel sol-gel synthesis of CeO<sub>2</sub> nanoparticles using Morinda citrifolia L. fruit extracts: structural and optical analysis*. Journal of Molecular Structure, 2021. **1231**: p. 129904.
- [12] Ramachandran, M., et al., *Role of surfactant on synthesis and characterization of cerium oxide (CeO<sub>2</sub>) nanoparticles by modified co-precipitation method*. International Research Journal of Engineering and Technology, 2017. **4**(9): p. 31-35.
- [13] Muthuvel, A., et al., *Synthesis of CeO<sub>2</sub> NPs by chemical and biological methods and their photocatalytic, antibacterial and in vitro antioxidant activity*. Research on Chemical Intermediates, 2020. **46**: p. 2705-2729.
- [14] Yadav, T. and O. Srivastava, *Synthesis of nanocrystalline cerium oxide by high energy ball milling*. Ceramics International, 2012. **38**(7): p. 5783-5789.
- [15] Farahmandjou, M., M. Zarinkamar, and T. Firoozabadi, *Synthesis of Cerium Oxide (CeO<sub>2</sub>) nanoparticles using simple CO-precipitation method*. Revista mexicana de física, 2016. **62**(5): p. 496-499.
- [16] Khadar, Y.S., et al., *Synthesis, characterization and antibacterial activity of cobalt doped cerium oxide (CeO<sub>2</sub>: Co) nanoparticles by using hydrothermal method*. Journal of Materials Research and Technology, 2019. **8**(1): p. 267-274.
- [17] Lee, J.-S. and S.-C. Choi, *Crystallization behavior of nano-ceria powders by hydrothermal synthesis using a mixture of H<sub>2</sub>O<sub>2</sub> and NH<sub>4</sub>OH*. Materials Letters, 2004. **58**(3-4): p. 390-393.
- [18] Feng, S.-H. and G.-H. Li, *Hydrothermal and solvothermal syntheses*, in *Modern inorganic synthetic chemistry*. 2017, Elsevier. p. 73-104.
- [19] Pathak, V., et al., *Synthesis, characterization and applications of cubic fluorite cerium oxide nanoparticles: a comprehensive study*. Results in Surfaces and Interfaces, 2023. **11**: p. 100111.

- [20] Sankar, J. and S.S. Kumar, *Synthesis and characterization of nano cerium oxide using hydrothermal technique*. Incas Bulletin, 2021. **13**(1): p. 173-181.
- [21] Shlapa, Y., et al., *Cerium dioxide nanoparticles synthesized via precipitation at constant pH: Synthesis, physical-chemical and antioxidant properties*. Colloids and Surfaces B: Biointerfaces, 2022. **220**: p. 112960.
- [22] Calvache-Muñoz, J., F.A. Prado, and J.E. Rodríguez-Páez, *Cerium oxide nanoparticles: Synthesis, characterization and tentative mechanism of particle formation*. Colloids and Surfaces A: Physicochemical and Engineering Aspects, 2017. **529**: p. 146-159.
- [23] Abd-Alghafour, N., I.H. Kadhim, and G.A. Naeem, *UV detector characteristics of ZnO thin film deposited on Corning glass substrates using low-cost fabrication method*. Journal of Materials Science: Materials in Electronics, 2022. **33**(31): p. 23888-23899.
- [24] Mamdooh, N.W. and G.A. Naeem. *Green synthesis, characterization and biological activity of Silver nanoparticles Using Ruta Leaf Extract*. in *Journal of Physics: Conference Series*. 2021. IOP Publishing.
- [25] Hashim, H.T., et al., *Preparation Nanostructured of Cu-Doped NiO Thin Films Using Spin Coating Method for Gas Sensors Applications*. Journal of Nanostructures, 2022. **12**(4): p. 882-891.
- [26] Mamdooh, N.W. and G.A. Naeem. *The effect of temperature on green synthesis of silver nanoparticles*. in *AIP Conference Proceedings*. 2022. AIP Publishing.
- [27] Jayakumar, G., A.A. Irudayaraj, and A.D. Raj, *Particle size effect on the properties of cerium oxide (CeO<sub>2</sub>) nanoparticles synthesized by hydrothermal method*. Mechanics, Materials Science & Engineering Journal, 2017. **9**(1).
- [28] Yu, R., et al., *Controlled synthesis of CeO<sub>2</sub> flower-like and well-aligned nanorod hierarchical architectures by a phosphate-assisted hydrothermal route*. The Journal of Physical Chemistry C, 2008. **112**(50): p. 19896-19900.
- [29] Kadhim, F.M., et al. *Synthesis of TiO<sub>2</sub>, CeO<sub>2</sub> and their composite nanostructures for gas sensor applications*. in *AIP Conference Proceedings*. 2021. AIP Publishing.
- [30] Ramaprasad, T., et al., *Effect of pH value on structural and magnetic properties of CuFe<sub>2</sub>O<sub>4</sub> nanoparticles synthesized by low temperature hydrothermal technique*. Materials Research Express, 2018. **5**(9): p. 095025.